

## Edge chirality determination of graphene by Raman spectroscopy

YuMeng You, ZhenHua Ni, Ting Yu, and ZeXiang Shen<sup>a)</sup>

*Division of Physics and Applied Physics, School of Physical and Mathematical Sciences, Nanyang Technological University, Singapore 637371, Singapore*

(Received 21 July 2008; accepted 30 September 2008; published online 22 October 2008)

Raman imaging of single layer micromechanical cleavage graphene was carried out. The intensity of disorder-induced Raman feature (*D* band at  $\sim 1350\text{ cm}^{-1}$ ) was found to be correlated to the edge chirality: it is stronger at the armchair edge and weaker at the zigzag edge. This shows that Raman spectroscopy is a reliable and practical method to identify the chirality of graphene edge and hence the crystal orientation. The determination of graphene chirality is critically important for fundamental study of graphene as well as applications of graphene-based devices. © 2008 American Institute of Physics. [DOI: 10.1063/1.3005599]

Graphene has attracted great attention not only because it is the ideal material to study the fundamental properties of two-dimensional nanostructures,<sup>1</sup> but also for its potential applications in future electronic devices.<sup>2</sup> The exceptionally high crystallization and unique electronic properties make graphene a promising candidate for ultrahigh speed nanoelectronics.<sup>3,4</sup> Graphene nanoribbons (GNRs) have been receiving remarkable attention.<sup>5–8</sup> It was predicted that GNR with certain edge chirality would open the bandgap<sup>5,6,9</sup> and show distinguish magnetic,<sup>7,8</sup> optical,<sup>10</sup> and superconductive<sup>11</sup> properties. All these peculiar properties are strongly dependent on the edge chirality (zigzag or armchair). Conventional methods such as transmission electron microscopy (TEM), X-ray diffraction, and scanning tunneling microscope are either destructive, very time consuming, or nearly impossible to locate such small regions of interest.<sup>12,13</sup> The increasing interests in graphene demand a fast and nondestructive method to determine the chirality of edges and the crystal orientation.

As a perfect single crystalline structure, the micromechanical cleavage graphene (MCG) sheet is also expected to have similar cleavage behaviors.<sup>14</sup> After studying hundreds of MCG pieces, we found that the angles between MCG edges have an average value equaling to multiples of  $30^\circ$ . Figure 1(a) shows the optical image of a typical MCG sheet and the angles between the edges as an example. Figure 1(b) shows the measurement of angles. It can be clearly seen that most of the angles are distributed around  $n \times 30^\circ$ , where  $n$  is an integer between 0 and 6. Such a distribution suggests that the carbon atoms along the graphene edges have either zigzag or armchair structures. It can be easily shown that when the angle between two adjacent edges is  $30^\circ$ ,  $90^\circ$ , or  $150^\circ$ , the two edges have different chiralities, i.e., one armchair and the other one zigzag. On the hand, when the angle is  $60^\circ$  or  $120^\circ$ , both edges have the same chirality (either zigzag or armchair). Recently, scanning electron microscopy and TEM results have actually shown that the edge of graphene is not ideally smooth.<sup>15</sup> For such edges, both kinds of chirality should exist. However, the majority of carbon atoms still

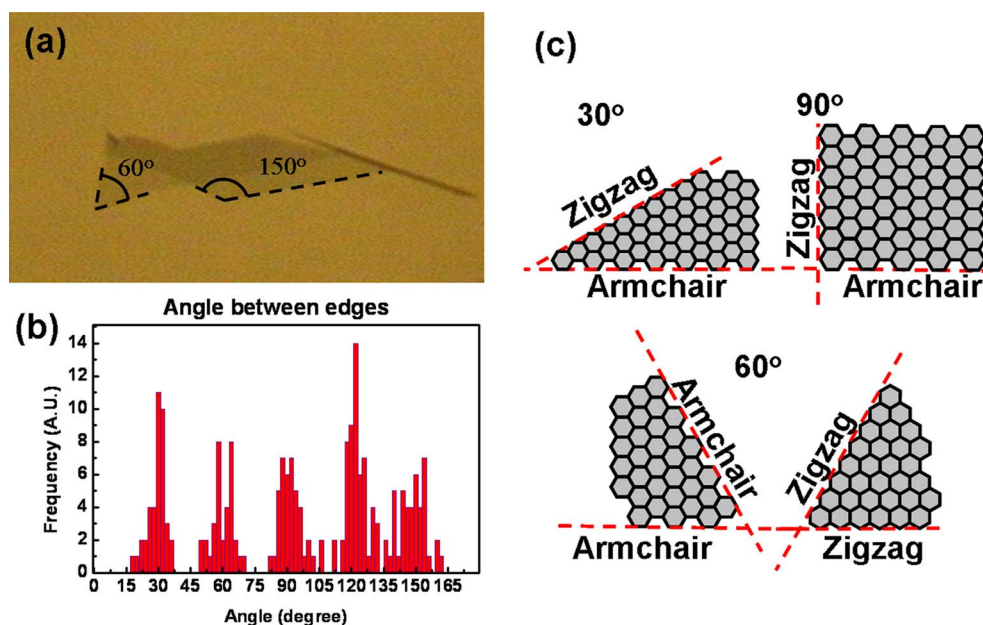


FIG. 1. (Color online) (a) Optical image of a typical MCG sheet and the angles between edges. (b) The statistical results of the angle measurements. The standard deviation is  $5.4^\circ$ . (c) Illustration of the relationship between angles and the chiralities of the adjacent edges.

<sup>a)</sup> Author to whom correspondence should be addressed. Electronic mail: zexiang@ntu.edu.sg.

have the same arrangement as the smooth one. Therefore, the angle and chirality of edges should result from a microscopic averaging effect, as the majority of the carbon atoms along the edge are arranged in one kind of chirality different from the other kind. As a result, the chirality we mentioned in this work is the average from the statistics.

As one of the most commonly used techniques to characterize carbon related materials, Raman spectroscopy plays a very important role in acquiring information on the physical, chemical, and even electronic properties of graphene and graphene based devices.<sup>16,17</sup> In this work, we are able to determine the edge chirality, hence the crystal orientation of graphene using the difference in intensity of the *D* band on the different chiralities of edges (stronger in armchair edges and weaker in zigzag edges). This provides an easy and non-destructive method to identify the edge chirality of graphene, which would help to speed up the practical applications of graphene nanoelectronic devices, such as GNR.

The MCG sheets are prepared using the common micro-mechanical cleavage method on a 300 nm SiO<sub>2</sub>/Si substrate, which provides a good optical contrast.<sup>18</sup> The Raman study was carried out using a WITec CRM200 confocal microscopy Raman system with a 100× objective lens (numerical aperture=0.95). The excitation light is 532 nm laser. Raman images were generated by scanning the sample with step size of 100 nm with a spatial resolution ~500 nm.

A piece of single layer graphene (SLG) is used as the sample. The number of layer has been determined by Raman spectroscopy as well as the contrast method.<sup>18,19</sup> There are three edges. The angle ( $\theta_1$ ) between edge 1 and 2 is 30° and the angle ( $\theta_2$ ) between edge 2 and 3 is 120°. Based on previous discussions, edge 1 and 2 should have different chiralities, and edge 2 and 3 have the same chirality. The main question here would be whether it is possible to determine the chirality of each edge. Here, Raman spectroscopy proves to be critically useful.

An SLG normally shows three major Raman bands as the *G* band around 1580 cm<sup>-1</sup>, a very weak *D* band around 1350 cm<sup>-1</sup> and a 2*D* band around 2670 cm<sup>-1</sup>,<sup>20</sup> as shown in Fig 2(d). The *G* band is related to the in-plane vibrational mode, which has been studied in detail in all the graphitic materials. The appearance of the *D* band and 2*D* band is related to the double resonance Raman scattering process, which consists of several steps. For the *D* band, an electron-hole pair is excited. Then the electron (or hole) is inelastically scattered by a phonon, following the elastic scattering of the electron (or hole) by a defect. Finally, the excited electron and phonon recombine.<sup>21</sup> For the 2*D* band, elastic scattering of the electron (or hole) in the above process is replaced by the second phonon.<sup>22</sup>

On the other hand, the edge structure of graphene, like a defect, is also necessary for the double resonance condition.<sup>23</sup> Such edge structure of highly ordered pyrolytic graphite (HOPG) have been studied by Cancado *et al.*<sup>23</sup> Pimenta *et al.*<sup>24</sup> They found that the *D* band that appears at the armchair edge of HOPG is much stronger than that at the zigzag edge. Their theoretical study was based on the model of SLG. After applying double resonance theory and considering the one-dimensional character of the edge they claimed that, the double resonance process can only be fulfilled at an armchair edge (stronger *D* band); while for a zigzag edge, the resonance process is forbidden (weaker or vanished *D*

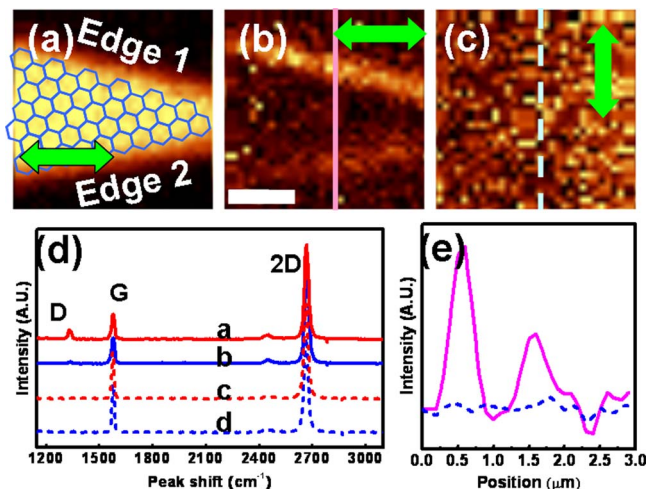


FIG. 2. (Color online) (a) Raman image constructed by the intensity of *G* band with the expected arrangement in blue. (b) and (c) are images constructed by the *D* band intensity with horizontal and vertical polarization, respectively. All images share the same scale bar as indicated in (b) which is 2  $\mu\text{m}$ . (d) Raman spectra taken from edge 1 (spectrum a), and edge 2 (spectrum b), with horizontal laser polarization. Spectra c and d were also collected from edges 1 and 2, respectively, with vertical laser polarization. (e) The solid and dotted lines represent the *D* band intensity profile (solid/dash) plotted along the solid line on (b) and the dashed line on (c), respectively.

band). Hence, this idea is used to distinguish the chirality of the graphene edge and we focus mainly on the *D* band of SLG in this work.

Raman images edge 1 and 2 are shown in Figs. 2(a)–2(c). The bright part in Fig. 2(a) corresponds to the appearance of the *G* band. The *G* band intensity is distributed uniformly over the whole graphene sheet, indicating the good quality of the sample. Figs. 2(b) and 2(c) show the *D* band intensity of graphene with laser polarization in the horizontal and vertical directions, respectively. From these images, we can see that the *D* band only appears at the edges and shows a very strong polarization dependence. We put the sample in this orientation to ensure that both edges (1 and 2) make the same angle with the laser polarization,  $\pm 15^\circ$  to the horizontal polarization and  $\pm 75^\circ$  to the vertical polarization. Therefore, the stronger *D* band intensity at edge 1 compared to that at edge 2 is not due to the polarization effect, but related to the carbon atom arrangement at the edge, i.e., the chirality.<sup>23</sup> The spectra collected from different spots in both polarizations are shown in Fig. 2(d). All of the spectra are recorded under the same conditions. Spectra a and b are recorded at edges 1 and 2, respectively, with horizontal laser polarization, which is almost parallel to the two edges. The *D* band intensity of edge 1 is 1.7 times of that of edge 2. Since this is not due to the polarization effect, we can now identify edge 1 as armchair edge while edge 2 as zigzag edge. Do note that the armchair or zigzag arrangement mentioned here for edges 1 and 2 should be a result of the majority of carbon atoms along the edge being arranged in one kind of chirality (either armchair or zigzag). This can be demonstrated in spectrum b of Fig. 2(d), where a weak *D* band can be observed. This suggests that in edge 2, there is still a small portion of carbon atoms in armchair arrangement. On the other hand, spectra c and d in Fig. 2(e) are recorded at edges 1 and 2, respectively, with a vertical laser polarization. Both spectra hardly show any *D* band because of the polarization effect. Raman images of SLG edges with different angles are compared in Fig. 3. In the case of 30°

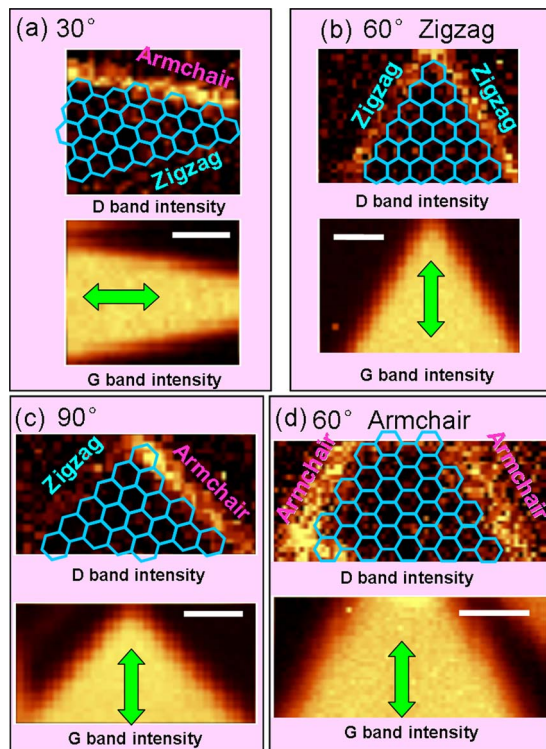


FIG. 3. (Color online) Raman imaging results from edges with angles (a)  $30^\circ$ , (b)  $60^\circ$  (zigzag), (c)  $90^\circ$ , and (d)  $60^\circ$  (armchair). The images constructed by the G band intensity show the positions and shapes of the SLG sheets. The laser polarization is indicated by the green arrows. The superimposed frameworks are guides for the eye indicating the edge chirality. Note that the chirality of (b) and (d) were determined by the other pair of edges (not shown) with  $30^\circ/90^\circ$  on the same piece of SLG. The scale bar is  $1 \mu\text{m}$ .

and  $90^\circ$ , edges show different *D* band contrast as they have different chiralities. On the other hand, in the case of  $60^\circ$ , a similar *D* band contrast is observed as the two edges have same chirality.

To rule out the possibility that the results of Raman imaging are caused by a difference in focusing or edge nonuniformity, we carried out a statistical analysis of the Raman intensities at each edge. For the SLG discussed in Fig. 2, it has three edges with an angle of  $30^\circ$  between edge 1 and 2 and  $120^\circ$  between edge 2 and 3. To compare the three edges under the same conditions, Raman imaging is carried out on each individual edge, with the laser polarization parallel to that edge (Raman images not shown). The *D* band obtained at different spots of the edge was then fitted using a Lorentzian function and the intensity image was plotted. We manually chose the data points along the edges with similar area ( $\sim 300 \text{ nm} \times 2 \mu\text{m}$ ) and calculated the average *D* band intensity generated from the edges. The average *D* band intensity from edge 1 (33.5) is obviously stronger than those from edges 2 (20.2) and 3 (22.0), which reveals that edge 1 is armchair and edges 2 and 3 are zigzag. This is consistent with the discussion in Fig. 2 about the chiralities of edge 1 and 2. Similar results were also obtained for other MCG sheets. We have in total measured nine pairs of edges with different angles,<sup>25</sup> and our Raman results agree well with expectation. For angles of  $30^\circ$  and  $90^\circ$ , two adjacent edges show different *D* band intensities, indicating they have different atomic arrangements at the edges. While for angles of

$60^\circ$  and  $90^\circ$ , two adjacent edges show similar *D* band intensities, showing that they have the same arrangement. The intensity ratio for the same chirality edge is around 1.0, while the difference for different chirality edges is greater than 1.6, which suggests that Raman spectroscopy is a practical and reliable method for determination of the graphene edge structure.

By knowing the edge arrangement, we can actually know the orientation of the whole graphene sheet. This is significant in the process of making graphene nanoconstriction using lithography techniques.<sup>26</sup> To conclude, we found that although the edges of MCG are not ideally smooth, they are on average predominantly either zigzag or armchair in nature. The defect-induced *D* band at the edges was found to be strongly polarization dependent, which is similar to that of graphite edges. This can be used to determine the crystallographic orientation of the MCG, which is important for the study of graphene and graphene-based devices.

- <sup>1</sup>K. S. Novoselov, A. K. Geim, S. V. Morozov, D. Jiang, Y. Zhang, S. V. Dubonos, I. V. Grigorieva, and A. A. Firsov, *Science* **306**, 666 (2004).
- <sup>2</sup>A. K. Geim and K. S. Novoselov, *Nature Mater.* **6**, 183 (2007).
- <sup>3</sup>K. I. Bolotin, K. J. Sikes, J. Hone, H. L. Stormer, and P. Kim, *Phys. Rev. Lett.* **101**, 096802 (2008).
- <sup>4</sup>K. I. Bolotin, K. J. Sikes, Z. Jiang, G. Fundenberg, J. Hone, P. Kim, and H. L. Stormer, *Solid State Commun.* **146**, 351 (2008).
- <sup>5</sup>X. L. Li, X. R. Wang, L. Zhang, S. W. Lee, and H. J. Dai, *Science* **319**, 1229 (2008).
- <sup>6</sup>M. Y. Han, B. Ozyilmaz, Y. B. Zhang, and P. Kim, *Phys. Rev. Lett.* **98**, 206805 (2007).
- <sup>7</sup>Y. W. Son, M. L. Cohen, and S. G. Louie, *Nature (London)* **444**, 347 (2006).
- <sup>8</sup>Y. W. Son, M. L. Cohen, and S. G. Louie, *Nature (London)* **446**, 342 (2007).
- <sup>9</sup>Y. W. Son, M. L. Cohen, and S. G. Louie, *Phys. Rev. Lett.* **97**, 216803 (2006).
- <sup>10</sup>L. Yang, M. L. Cohen, and S. G. Louie, *Nano Lett.* **7**, 3112 (2007).
- <sup>11</sup>A. G. Moghaddam and M. Zareyan, *Appl. Phys. A: Mater. Sci. Process.* **89**, 579 (2007).
- <sup>12</sup>J. C. Meyer, C. Kisielowski, R. Erni, M. D. Rossell, M. F. Crommie, and A. Zettl, *Nano Lett.* (to be published).
- <sup>13</sup>M. Ishigami, J. H. Chen, W. G. Cullen, M. S. Fuhrer, and E. D. Williams, *Nano Lett.* **7**, 1643 (2007).
- <sup>14</sup>S. Banerjee, M. Sardar, N. Gayathri, A. K. Tyagi, and B. Raj, *Appl. Phys. Lett.* **88**, 062111 (2006).
- <sup>15</sup>Q. K. Yu, J. Lian, S. Siriponglert, H. Li, Y. Chen, and S. S. Pei, arXiv:0804.1778v1 (2008).
- <sup>16</sup>M. S. Dresselhaus and P. C. Eklund, *Adv. Phys.* **49**, 705 (2000).
- <sup>17</sup>S. Reich and C. Thomsen, *Philos. Trans. R. Soc. London, Ser. A* **362**, 2271 (2004).
- <sup>18</sup>Z. H. Ni, H. M. Wang, J. Kasim, H. M. Fan, T. Yu, Y. H. Wu, Y. P. Feng, and Z. X. Shen, *Nano Lett.* **7**, 2758 (2007).
- <sup>19</sup>Y. Y. Wang, Z. H. Ni, Z. X. Shen, H. M. Wang, and Y. H. Wu, *Appl. Phys. Lett.* **92**, 043121 (2008).
- <sup>20</sup>A. C. Ferrari, J. C. Meyer, V. Scardaci, C. Casiraghi, M. Lazzeri, F. Mauri, S. Piscanec, D. Jiang, K. S. Novoselov, S. Roth, and A. K. Geim, *Phys. Rev. Lett.* **97**, 187401 (2006).
- <sup>21</sup>C. Thomsen and S. Reich, *Phys. Rev. Lett.* **85**, 5214 (2000).
- <sup>22</sup>Z. H. Ni, W. Chen, X. F. Fan, J. L. Kuo, T. Yu, A. T. S. Wee, and Z. X. Shen, *Phys. Rev. B* **77**, 115416 (2008).
- <sup>23</sup>L. G. Cancado, M. A. Pimenta, B. R. A. Neves, M. S. S. Dantas, and A. Jorio, *Phys. Rev. Lett.* **93**, 247401 (2004).
- <sup>24</sup>M. A. Pimenta, G. Dresselhaus, M. S. Dresselhaus, L. G. Cancado, A. Jorio, and R. Saito, *Phys. Chem. Chem. Phys.* **9**, 1276 (2007).
- <sup>25</sup>See EPAPS Document No. E-APPLAB-93-025843 for a table comparing *D* band intensity among the edges and supporting information. For more information on EPAPS, see <http://www.aip.org/pubservs/epaps.html>.
- <sup>26</sup>B. Ozyilmaz, P. Jarillo-Herrero, D. Efetov, and P. Kim, *Appl. Phys. Lett.* **91**, 192107 (2007).